

KINETIC MODEL OF THE XeF LASER

A.M. Boichenko, F.V. Karelin, and S.I. Yakovlenko

*Institute of General Physics
of the Russian Academy of Sciences, Moscow*

Received April 15, 1995

We present here a nonstationary kinetic model of the XeF (B → X) laser on a mixture of Ne, Xe, and NF₃ pumped with a source of hard ionization. The model presented enables a description of lasing parameters for emissions at different wavelengths (351 and 353 nm) as functions of the medium temperature. We also study here these lasing properties under conditions near the pump threshold.

1. INTRODUCTION

Among the plasma lasers,¹⁻³ the exciplex inerthaloid lasers are now the most powerful in the UV and VUV regions. The lasers on the exciplex molecules of KrF ($\lambda = 249$ nm), ArF ($\lambda = 193$ nm), XeCl ($\lambda = 308$), XeF ($\lambda = 351, 353$ nm) (Refs. 4-7) are particularly known in this group. The lasing transition in these molecules is the B → X transition, where the lower term, X, is loosely bound.

The most efficient are KrF lasers with the efficiency as high as 10% and, likely, ArF laser,⁸⁻¹¹ whereas the efficiency of XeF lasers is not so high (about 3%). However, this laser is interesting because of the lowest pumping threshold. In this connection, a possibility of using a nuclear pump for this laser is discussed.¹² From our point of view, the computer modeling is required before making experiments with the nuclear pump. The model experiments with electron beams of microsecond duration are also desirable.

The specific features of the XeF laser are related to the fact that the lasing takes place in it not only on the B → X transition but also on the C → A transition. Besides, the term X in XeF molecule lies in a sufficiently deep potential well. This results in relatively low efficiency and pronounced temperature dependence of the lasing characteristics. Note that the existing models of XeF (B → X) laser¹³⁻²³ do not take into account, or do it insufficiently correct, the temperature dependence of the rates of different kinetic reactions. In many papers only one efficient transition is considered rather than lasing at $\lambda = 351$ and 353 nm separately. Moreover, the models were compared with a very limited number of experiments including, as a rule, no more than one lasing experiment.

We, in this paper, construct a detailed nonstationary kinetic model enabling one to adequately describe the dependence of the basic laser characteristics (energy, efficiency, moment when lasing jumps from 353 to 351 nm, etc.) on the medium temperature as well as consider the operation of the XeF laser near the pump threshold.

2. KINETIC MODEL

For a more detailed consideration of the relaxation channels and kinetic modeling see Ref. 42. Let us briefly list here only some basic features of the model.

2.1. General characteristics of the model

In constructing the kinetic model we use our previous experience in modeling active media for exciplex lasers on the molecules of KrF,⁴ XeCl,^{4,24,25} ArF,¹⁰⁻¹¹ and others⁴ as a background.

The model includes balance equations for 38 plasma particles: Ne, Xe, NF₃, Ne⁺, Ne₂⁺, Ne₃⁺, Ne*, Ne**, Ne₂^{*(1,3Σ_u⁺)}, Xe⁺, Xe₂⁺, Xe*, Xe**, Xe₂^{*}, Xe₂^{**}, NeXe⁺, NeXe*, NF₃⁺, NF₂, NF, N, N⁺, N₂, N₂⁺, XeF(B), XeF(C), XeF(X), Xe₂F, F, F⁻, F⁺, F*, F₂, F₂⁺, NeF, F₂^{*}, e. The balance equations for a particle number take into account about 260 plasma-chemical reactions. In addition the model includes equations for the electron, T_e , and ion, T , temperatures, as well as equations for the intensity of laser radiation at two wavelengths. Altogether, we consider 40 equations in ordinary derivatives and one bond equation for electrons, representing the condition of plasma quasineutrality. Earlier, when studying the properties of laser active media, attention has mostly been focused on the electron temperature dependence of the reaction rates, since the lasing characteristics were, as a rule, weakly dependent on gas temperature, T . While studying XeF laser, we have tried to take into account properly the gas temperature. To this end, in this model, in contrast to the earlier models we consider, in addition to two excited exciplex states, B and C, of the XeF molecule, the two-wave lasing on B → X transition between different vibrational states.

Considered in Refs. 1-5 were the active media pumped with a source of a hard ionization, i.e. fast charged particles or short-wave photons. In this case the velocity distribution function of plasma electrons in different plasma-chemical reactions can be considered to be Maxwellian, and the effect of hard ionization can

be described in the balance equations for particle number and thermal balance by the ionization frequency, $v_i(s^{-1})$, and energy of the electron-ion pair formation, E_p . These parameters are convenient because they vary little within a wide range of medium density and temperature and depend only on the initial chemical composition of the medium. The computations have been made with the PLASER program package.⁴

2.2. Relaxation channels

The main portion of pumping energy goes into the ionization and the excitation of neon atoms. The Xe^+ ions are mainly produced in Penning reactions of the excited neon atoms with xenon.

The electrons produced, colliding with each other, form the Maxwell velocity distribution with the electron temperature essentially higher than the gas one. The electrons are cooled due to elastic and inelastic collisions with neutral particles.

The plasma electrons produce negative fluorine ions F^- in the dissociative sticking reaction with NF_3 and its derivatives. The exciplex molecules XeF^* are produced mainly due to three-particle recombination of F^- with Xe^+ ions. A small contribution comes from reactions of NF_3 with Xe^* and Xe^{**} . The trapping of Ne^+ , Ne_2^+ , and F^- with production of NeF^* molecule as well as Penning reaction of Ne^* atoms with NF_3 molecules are parasitic ways. The mixing of B and C states is mainly due to collisions with neon atoms and electrons.

2.3. Temperature dependence of the reaction rates

Let us note that temperature dependence of the reaction rates was considered in Refs. 19, 21, but the rates of binary reactions were taken there to be proportional to $T^{1/2}$ whereas those of triple reactions were taken proportional to T^{-n} , where $n \approx 1.5-3.5$, that seems to be not enough accurate.

The reaction rates of charged particle conversion were believed proportional to $T^{-3/4}$ in accordance with the Thomson model and those of neutral particle association – proportional to $T^{-1/3}$.

The temperature dependence of the rates of binary reactions of heavy particles was neglected. With $T_g \approx T_e \approx 1$ eV, the rates of dissociative recombination behave as T^{-n} , where $n \approx 1-2$ (Ref. 26), with $T_g < T_e$ they behave as $T_e^{-\alpha}$, $\alpha \approx 0.5$ ($T \approx 300$ K) (Ref. 7). That is why at temperatures $T_g \approx 300-800$ K and $T_e \approx 1.5$ eV, we usually consider, the rates of dissociative recombination were taken as $k \sim T_e^{-\alpha} T_g^{-1}$, where $\alpha \approx 0.5$ and it depends on the kind of a molecular ion.

The rates of triple ion-ion recombination were determined in accordance with the Flannery theory.^{7,27,28}

The vibrational relaxation was taken to be fast enough, and, correspondingly, vibrational degrees of

freedom of states B, C, and X of the XeF molecule are distributed according to the Boltzmann law.

In a kinetic model, we used the total population of the $XeF(X)$ state. The rate of its dissociation was found using the expression

$$k_{\text{diss}} = 5 \cdot 10^{-10} T^{-0.27} e^{-0.184/T} (1 - e^{-0.0279/T})$$

and the rate of association was found from the expression

$$k_{\text{as}} = 0.5 \cdot 10^{-33} T^{-1.77} e^{-0.039/T} (1 - e^{-0.0279/T})$$

2.4. Emission

The emission of each laser component was considered based on kinetic equations for populations N_a and N_b of the working levels (subscripts a and b correspond to the lower and upper levels, respectively):

$$\begin{aligned} \frac{dN_a}{dt} = & -(K_a + \sigma_{ba}^{ph} I/h\omega) N_a + \\ & + (K_{ab} + \sigma_{ab}^{ph} I/h\omega) N_b + D_a; \end{aligned} \quad (1a)$$

$$\begin{aligned} \frac{dN_b}{dt} = & -(K_b + \sigma_{ba}^{ph} I/h\omega) N_a + \\ & + (K_b + \sigma_{ab}^{ph} I/h\omega) N_b + D_b; \end{aligned} \quad (1b)$$

Here σ_{ba}^{ph} and σ_{ab}^{ph} are the cross sections of $a \rightarrow b$ and $b \rightarrow a$ transitions; $h\omega$ is the energy of a radiation quantum being involved into the amplification.

We used 0-dimensional model for volume-averaged intensity of laser radiation:

$$\frac{dI}{dt} = (c\kappa - \gamma) I + cQ. \quad (2)$$

where c is the speed of light; $\gamma = (c/2L)\ln(1/R_1R_2)$ is the reciprocal photon lifetime in the cavity;

$$\kappa = \sigma_{ba}^{ph} (N_b - g_b N_a/g_a) - \sum \sigma_{X(m)}^{ph} [X(m)]$$

is the radiation gain factor; $\sigma^{ph}x(m)$ is the cross section of radiation absorption by $x(m)$ particles.

Equation (2) enters into the general set of equations together with other equations of the particle number balance. Equations (1) were considered for the radiation intensity I_1 , corresponding to vibronic transitions B, $v \rightarrow X$, v' : ($v = 0 \rightarrow v' = 2$; $1 \rightarrow 4$) at $\lambda = 351$ nm and for the intensity I_2 at $\lambda \approx 353$ nm ($0 \rightarrow 3$). In principle, the transition $1 \rightarrow 6$ also may contribute into the radiation at $\lambda = 353$ nm, but we ignore it. Since the total populations of XeF (B) and XeF (X) states were used in the model then when obtaining the gain factors κ^+ at these wavelengths, these populations were multiplied by the Boltzmann factor of the vibrational level, from which the absorption or amplification occurs.

We use the following expressions for the gain factors:

$$\begin{aligned} \kappa_{1,2} &= \kappa_{1,2}^+ - \kappa_{1,2}^-; \\ \kappa_1^+ &= \sigma_1^{ph} \{ [\text{Xe F(B)}]_{v=0} - [\text{Xe F(X)}]_{v=2} \} + \\ &+ [\text{Xe F(B)}]_{v=1} - [\text{Xe F(X)}]_{v=4} \} = \\ &= \sigma_1^{ph} \{ [\text{Xe F(B)}] [g_B(v=0) + g_B(v=1)] - \\ &- [\text{Xe F(X)}] [g_X(v=2) + g_X(v=4)] \}; \\ \kappa_2^+ &= \sigma_2^{ph} \{ [\text{Xe F(B)}]_{v=0} - [\text{Xe F(X)}]_{v=3} \} = \\ &= \sigma_2^{ph} \{ [\text{Xe F(B)}] g_B(v=0) - [\text{Xe F(X)}] g_X(v=3) \}; \\ \kappa_{1,2}^- &= \sum_m \sigma_{1,2,m}^- [X(m)], \end{aligned}$$

where the summation is over all radiation-absorbing components, except for XeF(X) molecule, which is already taken into account in $\kappa_{1,2}^+$; $\sigma_{1,2,m}^-$ are the absorption cross sections of these components. The absorption cross sections were mainly believed temperature-independent. Temperature dependences of the absorption cross sections of Ne_2^* , Ne_2^+ , NeXe^+ , Xe_2^+ , F_2^* presented in Ref. 17 are within the values obtained

in calculations and different experiments, so we used them too. The values of ω_e^A and energy of vibrational levels, $E^A(v)$, for the Boltzmann factors

$$g_A(v) = \frac{\exp(-(E^A(v) - E^A(0))/T)}{1/[1 - \exp(-\hbar \omega_e^A/T)]}$$

$A = B, X$, were taken from Refs. 29 and 30. The cross sections of stimulated emission $\sigma_{1,2}^{ph}$ may differ a little,²¹ but we took them equal $\sigma_{1,2} = 4.57 \cdot 10^{-16} \text{ cm}^2$ according to Ref. 31, assuming the lifetime of the B state to be equal to 14 ns.

3. COMPARISON WITH EXPERIMENTS

The first note describing the operation of XeF (B → X) laser was published in Ref. 32. The improvement of laser characteristic due to replacement of F₂-containing mixtures by NF₃-containing ones was discovered in Ref. 33, whereas the improvement due to replacement of argon as a buffer gas by neon was discovered in Refs. 34 and 35. Temperature dependence of efficiency was revealed in Ref. 36.

The comparison of some calculated characteristics with the experimental ones is presented in Figs. 1–3 and Tables I–III. For a more detailed comparison see Ref. 42.

TABLE I. Experimental⁴¹ and calculated efficiency ($\lambda = 353 \text{ nm}$) at different pumping power.

Pumping power, kW/cm ³	Experiment (Ref. 41)		Theory (this work)	
	Optimum, %	Laser intrinsic efficiency, %	Optimum, %	Laser intrinsic efficiency, %
36	80	1.5	87.5	1.75
44	90	1.7	82	1.91
60	90	2	76.5	2.09

In calculations we used $[\text{Ne}] = 8.07 \cdot 10^{19} \text{ cm}^{-3}$, $[\text{Xe}] = 2 \cdot 10^{17} \text{ cm}^{-3}$ (5.7 Torr), $[\text{NF}_3] = 4 \cdot 10^{16} \text{ cm}^{-3}$ (1.1 Torr), corresponding to experimental conditions. Ionization frequencies $\nu = 75, 92, \text{ and } 138 \text{ s}^{-1}$ correspond to the pumping power $\dot{W} = 36, 44, \text{ and } 60 \text{ kW/cm}^3$, and $\gamma = 2 \cdot 10^7, 3 \cdot 10^7, \text{ and } 4 \cdot 10^7 \text{ s}^{-1}$ correspond to reflection coefficients $R = 87.5, 82, \text{ and } 76.5\%$.

TABLE II. Comparison of the ratio (per cent) of energy emitted at different wavelengths with the experimental data⁴⁰ at a pressure of 3 Amagat units.

$\lambda, \text{ nm}$	$T = 300 \text{ K}$		$T = 425 \text{ K}$		$T = 464 \text{ K}$	$T = 476 \text{ K}$
	Theory	Ref. 40	Theory	Ref. 40	Theory	
353	98.7%	77%	88%	53%	60%	18%
351	1.3%	7%	12%	45%	40%	82%

In calculation we used the rectangular pumping pulse with duration $\tau = 550 \text{ ns}$ and the following values: $[\text{Xe}] = 8 \cdot 10^{17} \text{ cm}^{-3}$, $[\text{NF}_3] = 10^{17} \text{ cm}^{-3}$, that correspond to theoretically optimal concentrations at $T = 300 \text{ K}$, and $\nu = 586 \text{ s}^{-1}$. Every time we used $\gamma = 1.6 \cdot 10^8 \text{ s}^{-1}$ ($R \approx 35\%$). This value of R was optimal in calculations and in the experiment. The ionization frequency $\nu = 628 \text{ s}^{-1}$ corresponds to pumping power $\dot{W} = 300 \text{ kW/cm}^3$.

TABLE III. The dependence of the total ($\lambda = 351, 353 \text{ nm}$) efficiency of lasing on the composition (per cent) and the initial temperature of the medium at the total pressure of 3 Amagat units.

	Ne/Xe/NF ₃	T = 300 K		T = 350 K		T = 400 K		T = 450 K	
		Ref. 38	This work						
A	99.35/0.50/0.15	0.90±0.18	1.05	1.20±0.15	1.63	1.8±0.2	1.92	2.0±0.2	2.19
B	BAL/6Torr/2Torr	1.25±0.15	1.25	1.35±0.15	1.51	1.6±0.2	1.67	1.6±0.2	1.85
C	99.425/0.5/0.075	1.35±0.15	1.36	1.45±0.15	1.9	2.3±0.2	2.17	2.5±0.2	2.43
D	99.675/0.25/0.075	1.25±0.15	1.3	1.35±0.15	1.55	1.7±0.2	1.69	1.7±0.2	1.86

The ionization frequency $\nu = 188 \text{ s}^{-1}$ ($W = 90 \text{ kW/cm}^3$), $\gamma = 1.04 \cdot 10^8 \text{ s}^{-1}$ ($R = 50\%$). In Ref. 38, from which the experimental data were borrowed, the pumping duration was not specified. In our calculations we used $\tau_{1/2} = 1.2 \mu\text{s}$.

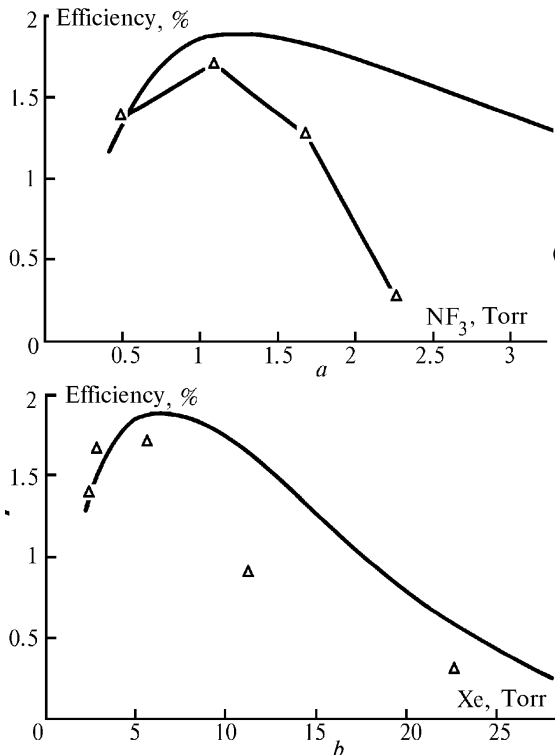


FIG. 1. The lasing efficiency at $\lambda = 353 \text{ nm}$ as a function of partial pressure of NF₃ with $[\text{Xe}] = 2 \cdot 10^{17} \text{ cm}^{-3}$ (5.7 Torr) (a) and Xe with $[\text{NF}_3] = 4 \cdot 10^{16} \text{ cm}^{-3}$ (1.1 Torr) (b): experimental⁴¹ (Δ) and calculated data (—). We used the ionization frequency $\nu = 92 \text{ s}^{-1}$ ($\dot{W} = 44 \text{ kW/cm}^3$), rectangular pumping pulse of $\tau = 4.25 \mu\text{s}$ duration, $[\text{Ne}] = 8.07 \cdot 10^{19} \text{ cm}^{-3}$, and $\gamma = 3 \cdot 10^7 \text{ s}^{-1}$ — the theoretically optimal for the given pumping power ($R \approx 80\%$).

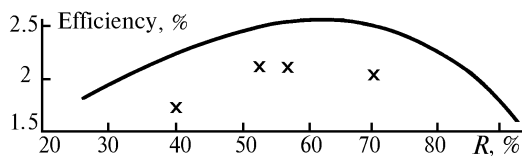


FIG. 2. XeF laser efficiency as a function of reflection coefficient R at $[\text{Ne}] = 8.07 \cdot 10^{19} \text{ cm}^{-3}$, $[\text{Xe}] = 4 \cdot 10^{17} \text{ cm}^{-3}$, $[\text{NF}_3] = 10^{17} \text{ cm}^{-3}$, $\nu = 276 \text{ s}^{-1}$ ($\dot{W} = 132 \text{ kW/cm}^3$), rectangular pumping pulse, $\tau = 1.15 \mu\text{s}$, $T = 300 \text{ K}$: experiment³⁹ (\times) and calculation (—).

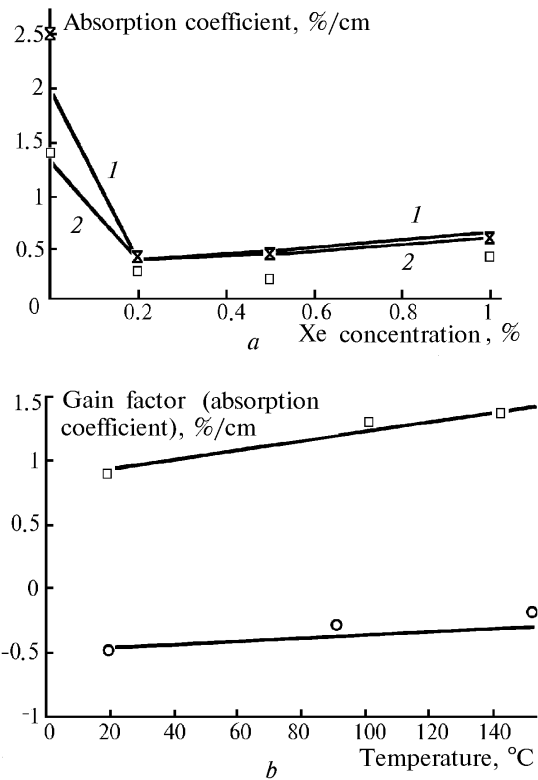


FIG. 3. a) The absorption coefficients in N₂/Xe mixture as functions of Xe concentration at $\lambda = 351 \text{ nm}$ and $p = 4 \text{ atm}$: experiment,³⁷ $T = 300 \text{ K}$ (\times), experiment,³⁷ $T = 423 \text{ K}$ (\square), calculation, $T = 300 \text{ K}$ (0.026 eV) (1), and calculation, $T = 423 \text{ K}$ (0.0364 eV) (2). The calculated absorption coefficients are presented for the time moments when they are maximum in absolute value ($t \approx 1.3 \mu\text{s}$), $\nu = 223 \text{ s}^{-1}$, $\tau_{1/2} = 1.2 \cdot 10^{-6} \text{ s}$;

b) the gain factors at $\lambda = 351 \text{ nm}$ for the Ne: 0.2Xe: 0.06NF₃ mixture: experiment³⁷ (\square) and calculation (—) and absorption coefficients for the mixture Ne:0.06NF₃ at $\lambda = 351 \text{ nm}$: experiment³⁷ (\circ) and calculation (—) vs. temperature ($^{\circ}\text{C}$) at $p = 4 \text{ atm}$ ($[\text{Ne}] = 1.08 \cdot 10^{20} \text{ cm}^{-3}$), $\nu = 223 \text{ s}^{-1}$, $\tau_{1/2} = 1.2 \cdot 10^{-6} \text{ s}$. The calculated gain factors and absorption coefficients are presented for the time moments when they are maximum in absolute values ($t \approx 1.3 \mu\text{s}$).

4. XeF LASER BEHAVIOR NEAR THE THRESHOLD

The most optimal operating mode of exciplex lasers corresponds to the pumping power about units of MW/cm³ and the pressure of several atmospheres. Such a pumping power is usually available from electron beams or volume discharge. It would be of practical interest to have a possibility of using the exciplex active media under the conditions of nuclear pumping, when the energy of nuclear reaction products goes into the laser active medium without any transformations.^{2,43,44} In this case, as was already mentioned, it might be reasonable to consider the mixture Ne–Xe–NF₃ as the medium with the lowest threshold among the active media based on halogenides of the inert gases.^{12,22,45}

Let us note that XeF laser behavior was studied in Ref. 22, but it was neglected there that the lower working state is bound. Moreover, the kinetics of active medium was considered as temperature independent and only one effective laser transition was taken into account. In addition, the comparison with experiments made in Ref. 22 is little informative.

As was mentioned above, the emission occurs at several lines, the strongest of them are $\lambda = 351$ and 353 nm, and both the total emitted energy and the energy corresponding to each λ depend now on the temperature of the gas mixture.

To describe the laser with nuclear pumping, the model must describe the above mentioned peculiar features. The matter is that although in nuclear pumping the power of energy contribution is low, the duration of energy input may be long (≈ 1 ms). As a result, the medium temperature also may change markedly during the pumping. In our kinetic model presented here, we tried to properly take into account these features.

Presented below are the dependences of different characteristics on the ionization frequency. The ionization frequency is related to the power W , contributed into the gas, via the relation

$$W = \nu E_{\text{pair}} N,$$

where ν is the ionization frequency, E_{pair} is the energy of a buffer gas pair, and N is the concentration of the buffer gas.

In the case of a foil pumping, the energy release in a gas can be related to the density of neutron flux by the relation

$$W = E_g \Phi_T \sigma_f N_5 \varepsilon V_{\text{foil}}/V_{\text{gas}},$$

where E_g is the energy of fission fragments; Φ_t is the density of neutron flux, σ_g is the cross section of ²³⁵U fission, N_5 is the ²³⁵U nucleus concentration, ε is the efficiency of fission energy transfer to gas (see, e.g., Ref. 46), V_{foil} and V_{gas} are the foil and gas volumes.

So the ionization frequency is related to the density of neutron flux via the relation:

$$\nu = \frac{E_g \Phi_T \sigma_f N_5 \varepsilon V_{\text{foil}}}{E_{\text{pair}} N V_{\text{gas}}}. \quad (3)$$

The specific values of the coefficients depend on the following parameters: neutron spectrum, medium composition and pressure, channel diameter, composition and thickness of the uranium coat, i.e. they are mainly governed by the construction features of the pump source. Therefore below we will describe the near-threshold characteristics of Ne–Xe–NF₃ laser as a function of the universal parameter ν , the transition from which to real neutron-physical parameter of specific nuclear-energy setups using Eq. (3) is not a heavy problem.

For efficient operation, the Ne–Xe–NF₃ mixture needs for high buffer gas pressure, however it does not always conform to the capabilities of nuclear pumping. In practice the thickness of the channel used, d , cannot be greater than several centimeters. Thus for $d = 2$ cm from the condition of the most efficient energy input it can be obtained that the pressure of mixture must be below 1 atm (Refs. 46 and 47).

The calculations have been made for the pumping duration at half-maximum $\tau_{1/2} = 1, 0.4, 0.2,$ and 0.1 ms, that are characteristic of existing setups and those under development. As expected, the optimal concentrations of Xe and NF₃ increase with increasing pump power. Optimization has been carried out in total energy emitted. The optima in total ($\lambda = 351$ and 353 nm) energy and efficiency are practically the same. For $\tau_{1/2} \leq 0.1$ ms the dependence of optimal concentrations of Xe and NF₃ on the ionization frequency changes its form, it becomes practically linear. Optimal value of γ drops with decreasing ionization frequency that is natural and corresponds to the increase in the mirror reflection coefficient. Note, however, that for ordinary cavities ($l < 1$ m) optimal values of r , corresponding to the ionization frequency lying immediately near the threshold, differ a little from unity and can hardly be realized in practice.

For the pump duration $\tau_{1/2} > 100 \mu\text{s}$ at the ionization frequency studied the total energy emitted increases, under optimal conditions, with increasing energy contribution (Fig. 4), whereas the total efficiency is optimal for ν in the range 10–30 s⁻¹ (Fig. 4b). The optimal value of ν decreases with decreasing pump duration $\tau_{1/2}$. With increasing temperature of the gas mixture the lasing spectrum is tuned that leads to a relative growth in the contribution to emission at $\lambda = 351$ nm as compared to that at $\lambda = 353$ nm (see Section 3). The same pattern can be seen here too. For $\tau_{1/2} = 1$ and 0.4 ms the total efficiency practically coincides with the efficiency at $\lambda = 351$ nm; for shorter $\tau_{1/2}$ the smooth tuning of emission from $\lambda = 353$ to $\lambda = 351$ nm takes place with the increase of pumping power (Fig. 4c).

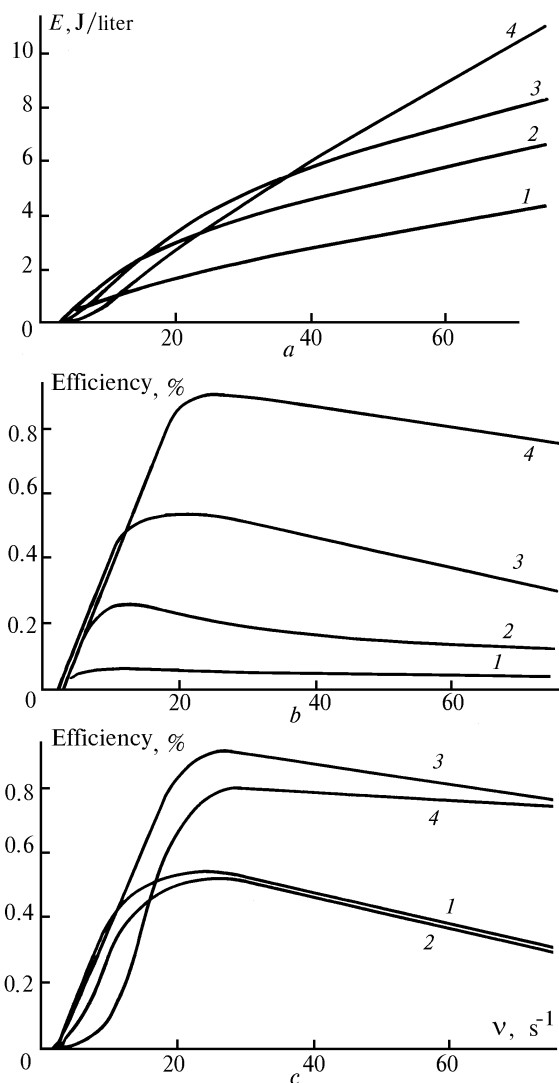


FIG. 4. a) Total (at $\lambda_1 = 351$ and $\lambda_2 = 353$ nm) emitted energy vs ionization frequency in optimal mode of lasing, the Ne–Xe–NF₃ mixture, $p = 1$ atm, for the pump duration at half-maximum $\tau_{1/2} = 1$ (curve 1), 0.4 (curve 2), 0.2 (curve 3), and 0.1 ms (curve 4);

b) total (at λ_1 and λ_2) efficiency vs ionization frequency in the optimal mode of lasing, the Ne–Xe–NF₃ mixture, $p = 1$ atm, for the pump duration at half-maximum $\tau_{1/2} = 1$ (curve 1), 0.4 (2), 0.2 (3), and 0.1 ms (4);

c) efficiency at different λ vs ionization frequency in optimal mode of lasing, the Ne–Xe–NF₃ mixture, $p = 1$ atm: $\tau_{1/2} = 0.2$ ms and $\lambda = \lambda_1 + \lambda_2$ (curve 1), $\tau_{1/2} = 0.2$ ms and $\lambda = \lambda_1$ (2), $\tau_{1/2} = 0.1$ and $\lambda = \lambda_1 + \lambda_2$ (3), and $\tau_{1/2} = 0.1$ ms and $\lambda = \lambda_1$ (4).

5. CONCLUSION

The detailed nonstationary kinetic model of Ne–Xe–NF₃ laser (B → X transition, $\lambda = 351$ and 353 nm) has been constructed. The characteristic feature of a XeF

laser that differs it from other inert–haloid lasers is the fact that gas temperature affects markedly the operation of this laser. The emission corresponds to bound–bound transitions, as a result, instead of a single band, two emission bands ($\lambda_1 = 351$ and $\lambda_2 = 353$ nm) occur. However, for the mixture under consideration these two important circumstances have been allowed for only in Refs. 16–19. In so doing, possible increase in laser energy and efficiency with increasing temperature was shown only in Refs. 16 and 17. Noted in Refs. 18 and 19 was the kinetic model allowing for these two circumstances. As an example, Ref. 19 presents, without a comparison with the experiment, only the dependences of κ^- and $\kappa = \kappa^+ - \kappa^-$ on time and, indirectly, on temperature, since the temperature in this example changed as a function of time.

The model, presented in this paper, describes adequately not only coarse parameters, such as optimal values of cavity mirror reflection coefficients and those of reagent relative concentration, but also more fine dependences:

1. temperature dependence of energy, efficiency, gain factor and absorption coefficient;
2. radiant flux as a function of time and mixture composition;
3. moments of emission jumps from λ_1 to λ_2 and vice versa as a function of time.

Characteristics of XeF (B → X laser) in Ne–Xe–NF₃ mixture have been studied theoretically at pressure $p = 1$ atm with nuclear pumping and the duration of pump pulse $\tau_{1/2} = 0.1$ –1 ms near the lasing threshold. The presence of efficiency optimum has been revealed in the ionization frequency range $\nu = 10$ –30 s⁻¹. In spite of the dependence of the ionization frequency corresponding to optimal efficiency on the pumping pulse duration, the threshold value of ionization frequency is independent of it and equals 2.5–3 s⁻¹ (400–500 W/cm³). However, for such an ionization frequency the cavity mirror reflection coefficient must be practically equal to unity that can be hardly realized in practice and, consequently, checked. The data presented are also true for pumping with electron beams if their parameters (pump duration and ionization frequency) correspond to those presented in this paper.

REFERENCES

1. L.I. Gudzenko, L.A. Shelepin, and S.I. Yakovlenko, *Usp. Fiz. Nauk* **114**, 457 (1974).
2. L.I. Gudzenko and S.I. Yakovlenko, *Plasma Lasers* (Atomizdat, Moscow, 1978), 256 pp.
3. S.I. Yakovlenko, in: *Plasma Physics*, Vol. 3 (VINITI, Moscow, 1982).
4. S.I. Yakovlenko, ed., *Visible and Near UV Plasma Lasers* (Nauka, Moscow, 1989), 142 pp.
5. S.I. Yakovlenko, *Laser Phys.* **1**, No. 6, 565–589 (1991).

6. Ch.K. Rhodes, ed., *Excimer Lasers* (Springer-Verlag, Berlin, 1979).
7. I. McDaniel and W. Nigan, eds., *Gas Lasers* [Russian translation] (Mir, Moscow, 1986).
8. A. Mandl, *J. Appl. Phys.*, **59**, 1435 (1986).
9. Y.M. Lee, H. Kumagai, S. Ashidate, and M. Obaga, *Appl. Phys. Lett.* **52**, 1294 (1988).
10. A.M. Boichenko, V.I. Derzhiev, A.G. Zhidkov, and S.I. Yakovlenko, *Kvant. Elektron.* **19**, 486 (1992).
11. A.M. Boichenko, V.I. Derzhiev, and S.I. Yakovlenko, *Laser Phys.* **2**, 210 (1990).
12. G.N. Hays, D.A. McArthur, D.R. Neal, and J. Rice, *Appl. Phys. Lett.* **49**, 363 (1986).
13. T.G. Finn, L.J. Palumbo, and L.F. Champagne, *Appl. Phys. Lett.* **33**, 148 (1978).
14. T.J. Johnson, L.J. Palumbo, and A.M. Hinter, *IEEE J. Quant. Electr.* **15**, 289 (1979).
15. M.M. Mkrchyan and V.T. Platonenko, *Kvant. Elektron.* **6**, 1639 (1979).
16. J.A. Blauer, T.T. Yang, C.E. Turner, Jr., and D.A. Copeland, *Appl. Optics* **23**, 4352 (1984).
17. J.A. Blauer, T.T. Yang, C.E. Turner, Jr., and D.A. Copeland, *AIAA J.* **23**, 741 (1985).
18. T.J. Moratz, T.D. Saunders, and M.J. Kushner, *J. Appl. Phys.* **64**, 3799 (1988).
19. T.J. Moratz, T.D. Saunders, and M.J. Kushner, *Appl. Phys. Lett.* **54**, 102 (1989).
20. N. Nishida, T. Takashima, F.K. Tittel, F. Kannari, and M. Obara, *J. Appl. Phys.* **67**, 3932 (1990).
21. A.V. Abarenov, I.G. Persiantsev, A.T. Rakhimov, S.P. Rebric, Yu.S. Shugai, and N.V. Sultin, *IEEE J. Quant. Electr.*, No. 27, 1946 (1991).
22. S.A. Mishenko, B.B. Krynetskii, A.M. Prokhorov, B.P. Sapsai, V.V. Stepanov, and A.G. Zhidkov, *Laser Phys.*, No. 2, 19 (1992).
23. A.V. Dem'yanov, N.A. Dyatko, I.V. Kochetov, and A.P. Napartovich, in: *Proceedings of Branch Conference on Physics of Nuclear-Excited Plasma and Lasers with Nuclear Pumping* (Obninsk, 1992), Vol. 1, p. 252.
24. A.M. Boichenko, V.I. Derzhiev, A.G. Zhidkov, and S.I. Yakovlenko, *Kvant. Elektron.* **16**, 278 (1989).
25. A.M. Boichenko, V.I. Derzhiev, A.G. Zhidkov, and S.I. Yakovlenko, *Kratk. Soobshch. Fiz.*, No.9, 9 (1990).
26. B.M. Smirnov, *Ions and Excited Atoms in Plasma* (Atomizdat, Moscow, 1974).
27. M.R. Flannery and T.P. Yang, *Appl. Phys. Lett.* **32**, 327 (1978).
28. M.R. Flannery and T.P. Yang, *Appl. Phys. Lett.* **32**, 356 (1978).
29. J. Tellinghuisen, P.C. Tellinghuisen, G.S. Tisone, J.M. Hoffman, and A.K. Hays, *J. Chem. Phys.*, No. 68, 5177 (1978).
30. P.C. Tellinghuisen, J. Tellinghuisen, J.A. Coxon, J.E. Velazco, and D.W. Setser, *J. Chem. Phys.*, No. 68, 5187 (1978).
31. M. Rokni, J.M. Jacob, J.A. Mangano, and R. Brochu, *Appl. Phys. Lett.* **30**, 458 (1977).
32. C.A. Brau and J.J. Ewing, *Appl. Phys. Lett.* **27**, 435 (1975).
33. E.R. Ault, R.S. Bradford, Jr., and M.L. Bhaumik, *Appl. Phys. Lett.* **27**, 413 (1975).
34. J. Hsia, J.A. Mangano, M. Rokni, A. Hawryluk, and J.M. Jacob, in: *Proceedings of 30th Ann. Gaseous Electron. Conference* (1977).
35. L.F. Champagne and N.N. Harris, *Appl. Phys. Lett.* **31**, 513 (1977).
36. J.C. Hsia, J.A. Mangano, J.H. Jacob, and M. Rokni, *Appl. Phys. Lett.* **34**, 208 (1979).
37. L.F. Champagne, *Appl. Phys. Lett.* **35**, 516 (1979).
38. D.H. Burde, T.T. Yang, D.G. Harris, L.A. Pagh, J.A. Tillotson, C.E. Turner, Jr., and G.A. Merry, *Appl. Opt.* **26**, 2539 (1987).
39. A.E. Mandl and H.A. Hyman, *IEEE J. Quant. Electr.* **22**, 349 (1986).
40. L. Litzenberger and A. Mandl, *Appl. Phys. Lett.* **52**, 1557 (1988).
41. A. Mandl, *J. Appl. Phys.* **71**, 1630 (1992).
42. A.M. Boichenko, A.V. Karelin, and S.I. Yakovlenko, *Laser Phys.* **5**, No. 1 (1995) (in print).
43. R. Thom and R.T. Schneider, *AIAA J.*, No. 10, 400 (1972).
44. L.I. Gudzenko and S.I. Yakovlenko, *KSF*, No. 2, 14 (1974).
45. A.M. Boichenko, A.V. Karelin, O.V. Sereda, and S.I. Yakovlenko, *Lasers and Particle Beams*, No. 11, 655 (1993).
46. A.V. Karelin, O.V. Sereda, V.V. Kharitonov, K.R. Chikin, and F.Yu. Naumkin, *Atomnaya Energiya*, No. 61, 44 (1986).
47. A.M. Boichenko, A.V. Karelin, and S.I. Yakovlenko, *Kvant. Elektron.* **22**, No. 3 (1995) (in print).